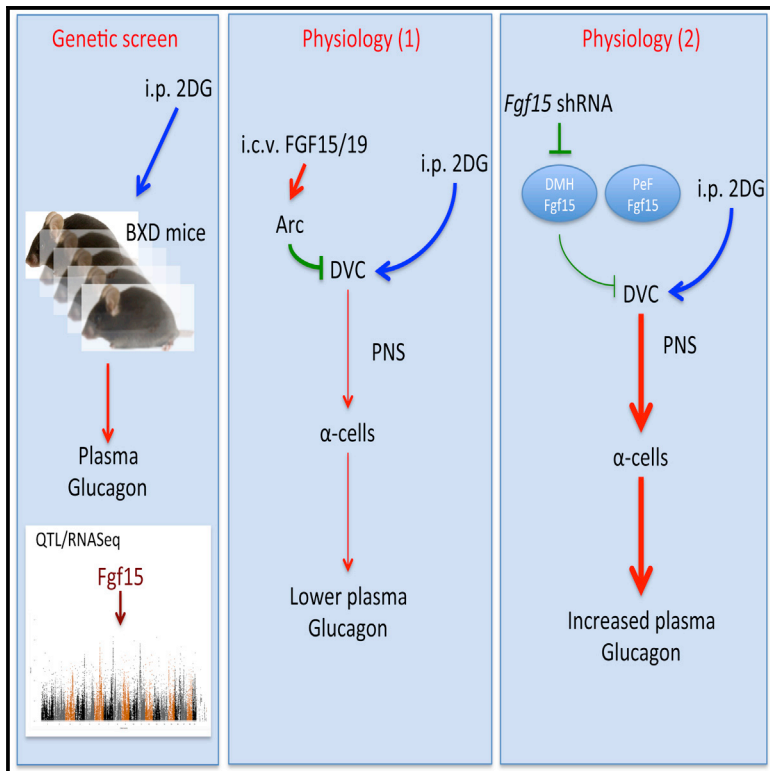


# Cell Reports

## A Genetic Screen Identifies Hypothalamic *Fgf15* as a Regulator of Glucagon Secretion

### Graphical Abstract



### Authors

Alexandre Picard, Josselin Soyer, Xavier Berney, ..., Frédéric Burdet, Mark Ibberson, Bernard Thorens

### Correspondence

bernard.thorens@unil.ch

### In Brief

Defects in the counterregulatory response to hypoglycemia and repeated hypoglycemic episodes are a major threat for insulin-treated diabetic patients. Picard et al. identify hypothalamic *Fgf15* as a, so far, unsuspected regulator of glucagon secretion that acts as an inhibitor of vagal activity using a genetic screen and physiological studies.

### Highlights

- Recombinant inbred mice screened for QTLs associated with glucagon secretion
- Combined QTL and transcriptomic analysis suggests a role for hypothalamic *Fgf15*
- *Fgf15* i.c.v. blunts neuroglucopenia-induced vagal nerve firing and glucagon secretion
- Silencing *Fgf15* mRNA in the dorsomedial hypothalamus increases glucagon secretion

### Accession Numbers

GSE87586



# A Genetic Screen Identifies Hypothalamic *Fgf15* as a Regulator of Glucagon Secretion

Alexandre Picard,<sup>1</sup> Josselin Soyer,<sup>1</sup> Xavier Berney,<sup>1</sup> David Tarussio,<sup>1</sup> Simon Quenneville,<sup>1</sup> Maxime Jan,<sup>2</sup> Eric Grouzmann,<sup>3</sup> Frédéric Burdet,<sup>2</sup> Mark Ibberson,<sup>2</sup> and Bernard Thorens<sup>1,4,\*</sup>

<sup>1</sup>Center for Integrative Genomics, University of Lausanne, 1015 Lausanne, Switzerland

<sup>2</sup>Vital-IT, Swiss Institute of Bioinformatics, 1015 Lausanne, Switzerland

<sup>3</sup>Service de Biomédecine, Laboratoire des Catécholamines et Peptides, Centre Hospitalier Universitaire Vaudois CHUV, 1011 Lausanne, Switzerland

<sup>4</sup>Lead Contact

\*Correspondence: [bernard.thorens@unil.ch](mailto:bernard.thorens@unil.ch)

<http://dx.doi.org/10.1016/j.celrep.2016.10.041>

## SUMMARY

The counterregulatory response to hypoglycemia, which restores normal blood glucose levels to ensure sufficient provision of glucose to the brain, is critical for survival. To discover underlying brain regulatory systems, we performed a genetic screen in recombinant inbred mice for quantitative trait loci (QTL) controlling glucagon secretion in response to neuroglucopenia. We identified a QTL on the distal part of chromosome 7 and combined this genetic information with transcriptomic analysis of hypothalami. This revealed *Fgf15* as the strongest candidate to control the glucagon response. *Fgf15* was expressed by neurons of the dorsomedial hypothalamus and the perifornical area. Intracerebroventricular injection of FGF19, the human ortholog of *Fgf15*, reduced activation by neuroglucopenia of dorsal vagal complex neurons, of the parasympathetic nerve, and lowered glucagon secretion. In contrast, silencing *Fgf15* in the dorsomedial hypothalamus increased neuroglucopenia-induced glucagon secretion. These data identify hypothalamic *Fgf15* as a regulator of glucagon secretion.

## INTRODUCTION

Glucose is the major source of metabolic energy for the brain. This requires that homeostatic processes maintain blood glucose concentration at a minimum of ~5 mM to ensure sufficient provision of glucose to the brain (Unger and Orci, 1981). Specialized glucose sensing cells present in peripheral locations, such as the hepatportal vein area, and in the CNS are activated by hypoglycemia and initiate a counterregulatory response to normalize glycemia (Chan and Sherwin, 2013; Frizzell et al., 1993; Jackson et al., 2000). This response is mediated by activation of the autonomous nervous system and the hypothalamo-pituitary-adrenal axis, leading to the release in the bloodstream of glucagon secreted by pancreatic alpha cells, and of catecholamines and glucocorticoids secreted by the

adrenal gland (Verberne et al., 2014). The combined action of these hormones promotes hepatic glucose production, lipolysis in the adipose tissue, suppression of insulin secretion, and inhibition of glucose uptake in muscle and fat. These actions restore normoglycemia and glucose flux to the brain (Verberne et al., 2014). The counterregulatory response to hypoglycemia is, thus, essential for survival.

In type 1 and type 2 diabetic patients treated with insulin, the counterregulatory response to hypoglycemia is progressively blunted causing occasional hypoglycemia. Antecedent hypoglycemic episodes then lead to a progressive loss of the hypoglycemia cognitive warning signals and to a reduced hormonal counterregulatory response. This condition, referred to as hypoglycemia associated autonomic failure (HAAF), augments the risks to develop hypoglycemic episodes of increased severity and is a major obstacle in the treatment of diabetes with insulin (Cryer, 2013).

Hypoglycemia detection in the brain occurs within specialized brain areas, mainly the hypothalamus and the brainstem (Marty et al., 2007; Ritter et al., 2011). These brain structures contain neuron subpopulations activated by an increase or a fall in extracellular glucose concentrations and which are referred to as glucose excited (GE) or glucose inhibited (GI) neurons, respectively (Routh, 2002). Identification of these neurons is based on electrophysiological recording of their firing activity assessed in acute brain sections or using dispersed neuron populations. The molecular mechanisms of glucose sensing by GE or GI neurons are diverse (Thorens, 2012). Glucose sensing by GE neurons involves proteins also controlling glucose-induced insulin secretion by pancreatic beta-cells such as *Glut2* (Lamy et al., 2014; Marty et al., 2007), glucokinase (Levin et al., 2008; Stanley et al., 2013), and the  $K_{ATP}$  channel (Evans et al., 2004; Miki et al., 2001). The  $Na^+$ /glucose co-transporters SGLT1 and SGLT3 may also contribute to glucose sensing by GE neurons (O'Malley et al., 2006). On the other hand, AMP-activated protein kinase (AMPK) plays a key role in activation of GI neurons by hypoglycemia (Alquier et al., 2007; McCrimmon et al., 2008). In contrast to AMPK and the  $K_{ATP}$  channel, which are present in all neurons, *Glut2*, glucokinase, and the SGLTs are present in specific, only partly overlapping neuronal subpopulations and may thus be used as markers of glucose-sensing neurons.

Identification of glucose sensing cells, in particular, those implicated in the adaptive response to hypoglycemia is of high importance to better understand the cause and possible management of HAAF. So far, the mechanisms of central glucose sensing have been explored based on the targeted analysis of genes known to be involved in glucose metabolism or signaling. Unbiased identification of genes controlling quantitative traits is, however, possible by screening genetic reference populations. The BXD recombinant inbred mice, which have been derived from the cross of DBA/2J and C57Bl6/J mice, form a particularly useful genetic reference population (Andreux et al., 2012; Chesler et al., 2004; Peirce et al., 2007; Rosen et al., 2007). These mice have been successfully used to identify genes involved in various physiological processes such as sleep (Franken et al., 2001), aging (Houtkooper et al., 2013), blood pressure (Koutnikova et al., 2009), or beta-cell function (Wong et al., 2013).

Here, we aimed at identifying genes involved in the counterregulatory response by screening a BXD mouse panel for the glucagon response to 2-deoxy-D-glucose (2DG)-induced neuroglucopenia. This led to the identification of a significant QTL on the distal part of chromosome 7. To identify the causal gene in the QTL, we hypothesized that this gene should be expressed in the hypothalamus, and that its expression should correlate with the glucagon trait. Combining QTL analysis and RNA-sequencing (seq) data, we identified hypothalamic *Fgf15* as the most likely candidate gene. The functional involvement of *Fgf15* was supported by showing that: (1) it is expressed in dorsomedial hypothalamus and perifornical neurons; (2) intracerebroventricular (i.c.v.) delivery of FGF19, the human ortholog of *Fgf15*, reduced 2DG-induced glucagon secretion through suppression of dorsal vagal complex neuron activation, and reduction of parasympathetic nervous activity; and (3) silencing of *Fgf15* in the DMH increased 2DG-induced glucagon secretion.

## RESULTS

### Genetic and Genomic Identification of Hypothalamic *Fgf15* as Regulator of Glucagon Secretion

We searched for genomic intervals associated with glucagon secretion induced by 2DG-induced neuroglucopenia in a panel of 36 BXD mouse strains. Groups of male mice were generated for each BXD strain and used when they reached 10 weeks of age. In a first experimental session, mice were injected intraperitoneally (i.p.) with a saline solution and blood was collected 30 min later for plasma preparation and storage. Two weeks later, the mice received an i.p. injection of 2DG and blood was collected and plasma prepared. Glucagon levels were measured by radioimmunoassay at the same time for all mice and the ratio between plasma glucagon after 2DG and NaCl injections was calculated. This trait varies by 3-fold between BXD strains (Figure 1A) with the lowest response (1.5-fold) detected in BXD49 and the highest (4.7-fold) in BXD50. This trait was due to differences in stimulated plasma glucagon levels rather than to differences in basal glucagonemia (Figure 1B); it was not correlated to differences in total pancreatic glucagon content across all the BXD strains (Figure 1C). This suggests that the variability in the secretion response results from differences in hypoglycemia

detection and signaling to pancreatic alpha cells rather than from differences in pancreatic glucagon stores.

Quantitative trait analysis identified a whole genome significant QTL at the distal part of the chromosome 7 (Figure 1D). The likelihood ratio statistic (LRS) peak is centered on marker rs2304086585 (LRS: 24.679; position: 151.6236 Mb) and flanked by markers c7.loc119 (position: 147.5303 Mb) and rs31652431 (position: 152.4411 Mb) (Figure 1E). This locus is ~5 Mb wide and it contains 128 genes; it explains 49 percent of the variance of the glucagon trait.

To narrow down the genes within the QTL, which could regulate glucagon secretion, we hypothesized, first, that these must be expressed in the hypothalamus where glucose sensitive neurons are located (Karnani and Burdakov, 2011; Ritter et al., 2011; Routh, 2010) and, second, that their level of expression must correlate with the glucagon phenotype, assuming that they are non-coding polymorphisms. We thus performed transcriptomic analysis of the hypothalamus from all the BXD strains using mice that had not undergone QTL screening to avoid a possible impact of 2DG treatment on gene expression. RNA was extracted from the hypothalamus of 3–6 mice for each strain and equal amounts of RNA from each mouse were pooled for transcript profiling by RNA sequencing analysis. We found that 65 of the 128 genes present in the Chr7 locus were expressed in the hypothalamus. The hypothalamic expression level of 11 genes was significantly correlated to the glucagon trait (Table 1). *Fgf15* mRNA was the most significantly, and negatively, correlated to the glucagon phenotype ( $r = -0.571$ ;  $p = 2.73 \times 10^{-4}$ ) (Table 1). The second gene in this table, which shows a similar high correlation with the trait as *Fgf15* is *Gm17685* ( $r = -0.562$ ;  $p = 3.58 \times 10^{-4}$ ). This encodes a long non-coding RNA transcribed in reverse orientation from exon 2 of *Fgf15*, and its expression is highly correlated with that of *Fgf15* ( $r = 0.824$ ;  $p = 6.68 \times 10^{-10}$ ). The correlation with the glucagon trait of the other nine genes (Table 1) showed at least 10-fold less significant p values. Furthermore, the *Fgf15* gene of the DBA/2J and C57BL/6 mice encodes the same amino acid sequence, supporting differential expression of this gene as a possible underlying cause of the glucagon trait. We thus selected to further investigate *Fgf15* expression in the hypothalamus and its role in the response to neuroglucopenia.

### Hypothalamic *Fgf15* Expression, Parasympathetic Activity, and Glucagon Secretion

Quantitative analysis of *Fgf15* expression in different brain nuclei showed highest expression in the hypothalamus (average cycle threshold [CT] of 28.7) and lower expression in the hippocampus, thalamus, and brainstem, with almost undetectable levels in the cerebellum and cortex (average CTs of 29.6, 30.1, 30.1, 34.2, and 34.5, respectively) (Figure 2A). Brain expression of *Fgf15* was, however, much lower than its expression in the ileum, its major site of expression (average CT of 21.1) (Figure 2A) (Inagaki et al., 2005). Expression of the *Fgf15* receptors *Fgfr1c*, *Fgfr4*, and of the co-receptor *Klotho beta* was found in all brain regions (Figures 2B–2D).

To determine the site of *Fgf15* expression, we performed in situ hybridization analysis on hypothalamic sections. As shown in Figures 2E–2I, *Fgf15* expression was found mainly in

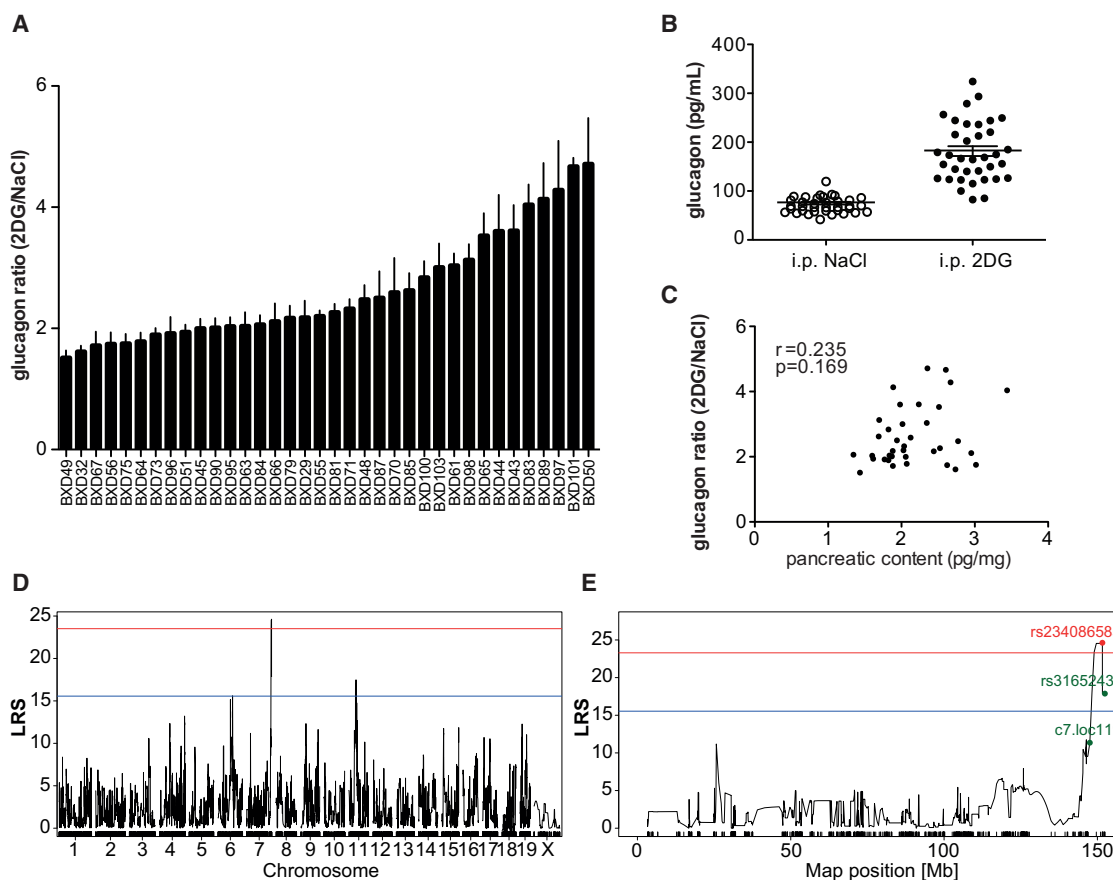


**Figure 1. A Locus on Chromosome 7 Controls Neuroglucopenia-Induced Glucagon Secretion**

- (A) Distribution of the glucagon ratio (2DG/NaCl) phenotype in the 36 BXD strains (n = 4–14 for each strain).  
 (B) Basal and neuroglucopenia-stimulated glucagonemia in the 36 BXD mouse strains. Each circle is the mean glucagonemia for each strain.  
 (C) Scatterplot representing the absence of correlation between the glucagon ratio (2DG/NaCl) phenotype and the total pancreatic glucagon content in BXD mice.  
 (D) Whole genome significant QTL on distal chromosome 7. The red line indicates the whole genome significance threshold ( $p \leq 0.05$ ). The blue line indicates the whole genome suggestive threshold ( $p \leq 0.63$ ).  
 (E) Localization of the locus between with a LRS peak on marker rs234086585.

the perifornical area (PeF; Figure 2E) and the dorsomedial hypothalamus (DMH; Figure 2G). In situ hybridization using a control probe derived from a bacterial gene, *DapB*, showed no staining (Figure 2H). No *Fgf15* transcripts were detected in the dorsal vagal complex of the brainstem (Figure 2I). Detection of *Fgf15* in ileal villi is shown for comparison (Figure 2J). Finally, double in situ hybridization of *Fgf15* and of the neuronal marker *NeuN* showed that *Fgf15* was expressed in neurons (Figures 2K and 2L).

To verify that *Fgf15* could regulate glucagon secretion through a central mechanism of action, we injected C57BL/6 mice i.c.v. with FGF19 (the human ortholog of *Fgf15*, which shows high stability in vivo and activates the same receptors; Owen et al., 2015) or an artificial cerebrospinal fluid (aCSF). Sixty min later, the mice received an i.p. injection of saline or 2DG. The glycemia was not modified by i.c.v. injections of saline or FGF19 (Figure 3A;  $t = 0$ ) and was similarly increased 30 min after i.p. 2DG injection in both groups of mice (Figure 3A). The plasma glucagon level in i.p. saline injected mice was unaffected by previous i.c.v.

FGF19 injection (Figure 3B). However, following 2DG-induced neuroglucopenia, the glucagon response was markedly lower in mice previously treated with i.c.v. FGF19 (Figure 3B). In these experiments, secretion of insulin, corticosterone, and epinephrine 30 min after i.p. saline or 2DG injections was not affected by previous i.c.v. FGF19 injection (Figures 3C–3E).

Next, we assessed hypothalamic *Fgf15* expression and 2DG-induced glucagon secretion in normal chow (NC) or high fat diet (HFD) fed mice, which show altered glucagon plasma levels (Burdulin et al., 2002). Mice fed a HFD for 4 weeks showed increased hypothalamic expression of *Fgf15* compared to NC fed mice (Figure 3F). When injected with 2DG, NC and HFD mice showed the same hyperglycemic response (Figure 3G). The basal glucagonemia of both groups of mice were the same, but the plasma glucagon response to 2DG was markedly reduced in HFD fed mice (Figure 3H). Thus, HFD feeding increased hypothalamic *Fgf15* expression and is correlated with reduced neuroglucopenia-induced glucagon secretion in agreement with the results of the genetic screen.

**Table 1. QTL Genes Expressed in the Hypothalamus and Correlated with the Glucagon Trait**

Gene <sup>a</sup>	Start	Strand	Length	Gene ID	NM ID	r <sup>b</sup>	p Value <sup>c</sup>
Fgf15	152.082436	+	4.42	14170	NM_008003	-0.571	2.73 × 10 <sup>-4</sup>
Gm17685	152.080465	-	2.902	NA		-0.562	3.58 × 10 <sup>-4</sup>
Ccnd1	152.115835	+	9.995	12443	NM_007631	0.472	0.00369
Ppfia1	151.66266	-	76.975	233977	NM_001195086	0.457	0.00509
Dhcr7	151.009071	-	25.244	13360	NM_007856	-0.456	0.00520
Cttn	151.621628	-	35.018	13043	NM_007803	0.440	0.00726
Kcnq1ot1	150.399016	-	83.437	63830	AK041889	-0.415	0.0119
Slc22a18	150.659659	+	25.578	18400	NM_001042760	-0.401	0.0153
Lrdd	148.624413	-	4.841	57913	NM_022654	-0.379	0.0228
Ifitm1	148.153327	+	2.399	68713	NM_001112715	-0.332	0.0482
Tmem80	148.514028	-	9.026	71448	NM_027797	0.331	0.0488

<sup>a</sup>Genes are listed according to the p value of the correlation between gene expression and the glucagon trait.

<sup>b</sup>r: Pearson's correlation coefficient between gene expression and the glucagon trait.

<sup>c</sup>p value: p value of the Pearson's correlation between gene expression and the glucagon trait.

To more directly determine whether the level of expression of *Fgf15* in the hypothalamus regulates glucagon secretion, we developed recombinant lentiviruses to express a control or an *Fgf15*-specific short hairpin (sh)RNA. Three shRNAs were designed to target the *Fgf15* sequence and were subcloned in lentiviral vectors. These were first tested in HEK293T cells cotransfected with an *Fgf15*-GFP expression plasmid. One vector induced efficient silencing of *Fgf15* mRNA and protein expression (Figures 4A–4C). This was used to generate a recombinant lentivirus, which effectively silenced *Fgf15* expression in transduction experiments (Figure 4D). This or a control lentivirus was then injected bilaterally in the DMH (Figure 4E). Two weeks later, the mice were injected i.p. with 2DG and plasma glucagon was measured 30 min later. The mice were then killed to verify the sites of virus injection. No difference in basal glycemia or in glycemic response to 2DG injection was observed between the two groups of mice (Figure 4F). However, neuroglucopenia-induced glucagon secretion was significantly increased (22%) in mice with correct bilateral DMH injection of the silencing lentivirus as compared to mice injected with the control lentivirus (Figure 4G) or mice injected with *Fgf15*-specific shRNA lentivirus outside of the DMH (Figure 4G, “missed”). Bilateral injection of the silencing lentivirus in the PeF (Figure 4H) did not impact glycemia before and 30 min after i.p. 2DG (Figure 4I), nor the neuroglucopenia-induced glucagon secretion (Figure 4H). Taken together, these data show that *Fgf15* expression by DMH neurons has a negative impact on neuroglucopenia-induced glucagon secretion.

Glucagon secretion during hypoglycemia is triggered by the activation of both parasympathetic and sympathetic branches of the autonomic nervous system (ANS) (Taborsky and Munding, 2012). As i.c.v. FGF19 decreased the glucagon response to 2DG-induced neuroglucopenia, but had no effect in non-injected or i.p. saline injected mice, we measured sympathetic and parasympathetic nerve activities in response to i.p. 2DG in mice, which had previously received i.c.v. aCSF or FGF19. Parasympathetic nerve activity showed no differences between groups in the basal state (Figure 5A). After 2DG injection, its

activity increased 2-fold in mice pre-treated with aCSF, but remained unchanged in mice pre-treated with FGF19 (Figure 5A). Sympathetic nerve activity showed no differences between the groups in the basal state or following 2DG injections (Figure 5B). Thus, i.c.v. injection of FGF19 inhibits 2DG-induced parasympathetic, but not sympathetic nervous activity.

The dorsal motor nucleus of the vagus (DMNX) is formed by the soma of the vagal neurons and is controlled by inputs from several brainstem and hypothalamic nuclei (Berthoud et al., 1990; Steinbusch et al., 2015). To investigate whether FGF19 influences these neurons directly or indirectly, we quantified the number of pERK1/2 (activated by FGF19 binding to its receptor) positive cells in the hypothalamus and the brainstem 30 min after i.c.v. aCSF or FGF19 injections. We observed an increased number of pERK1/2 positive cells in the arcuate nucleus (ARC) after i.c.v. FGF19 injection (Figures 5C and 5D). No increase in pERK1/2 positive cells was observed in other hypothalamic nuclei, in the dorsal vagal complex (DVC, which comprises the DMNX, the nucleus tractus solitarius [NTS], and the area postrema [AP]), nor in other brainstem areas. These results are consistent with a previous study (Marcelin et al., 2013) and suggest that the primary neurons involved in the effect of FGF19 are located within the ARC.

To determine whether FGF19 could control vagal neurons of the DVC in an indirect manner, we injected mice i.c.v. with aCSF or FGF19 and 1 hr later i.p. with NaCl or 2DG. Thirty min later, the mice were killed and brain sections prepared for *c-fos* expression analysis by in situ hybridization. Figures 5E and 5F show that i.p. 2DG induced a strong increase in *c-fos* expression in the NTS and the DMNX. However, in mice, which had previously received FGF19, 2DG-induced *c-fos* expression was markedly lower in both structures.

These data further support a role for central *Fgf15* in modulating the sensitivity of the DVC to 2DG-induced neuroglucopenia and in reducing the stimulation of vagal activity. They also support a role of *Fgf15* neurons in controlling the DVC through an indirect mechanism that first controls arcuate neurons activity.

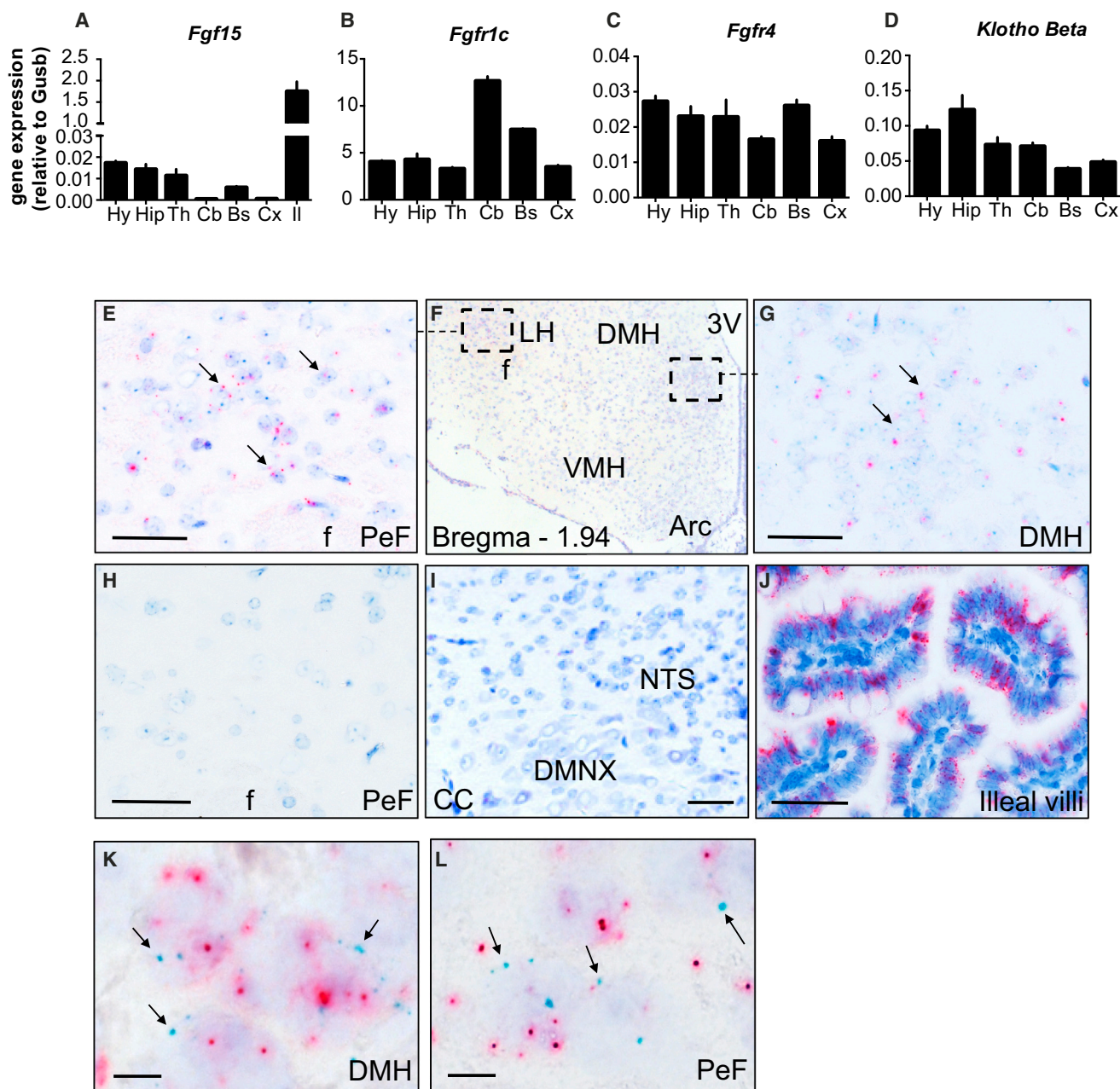


### Figure 2. *Fgf15* Expression in Adult CNS

(A–D) Expression level of *Fgf15*, *Fgfr1c*, *Fgfr4*, and *Klotho beta* in different brain structures and the ileum (n = 6–8). hypothalamus, Hy; hippocampus, Hip; thalamus, Th; cerebellum, Cb; brainstem, Bs; cortex, Cx; ileum, Il.

(E–J) In situ hybridization detection of *Fgf15* (red signal).

(E–J) PeF; representative section of hypothalamus at bregma –1.94 mm (F); DMH (G); negative control in PeF using *DapB* probes (H); brainstem with central canal (CC) DMNX and nucleus of the solitary tract (NTS) (I); and ileal villi (J). The scale bar represents 50  $\mu$ m.

(K and L) Double in situ hybridization of *Fgf15* (green dots) and *NeuN* (red dots) in PeF and DMH showing neuronal expression of *Fgf15*. The scale bar represents 10  $\mu$ m. The data are shown as mean  $\pm$  SEM.

## DISCUSSION

The present unbiased approach identified hypothalamic *Fgf15* as a negative regulator of glucagon secretion in response to neuro-

glucopenia. In situ hybridization revealed that *Fgf15* is expressed by a subgroup of neurons of the DMH and PeF. Physiological studies showed that i.c.v. injection of FGF19 reduced, whereas shRNA mediated silencing of *Fgf15* in the DMH increased

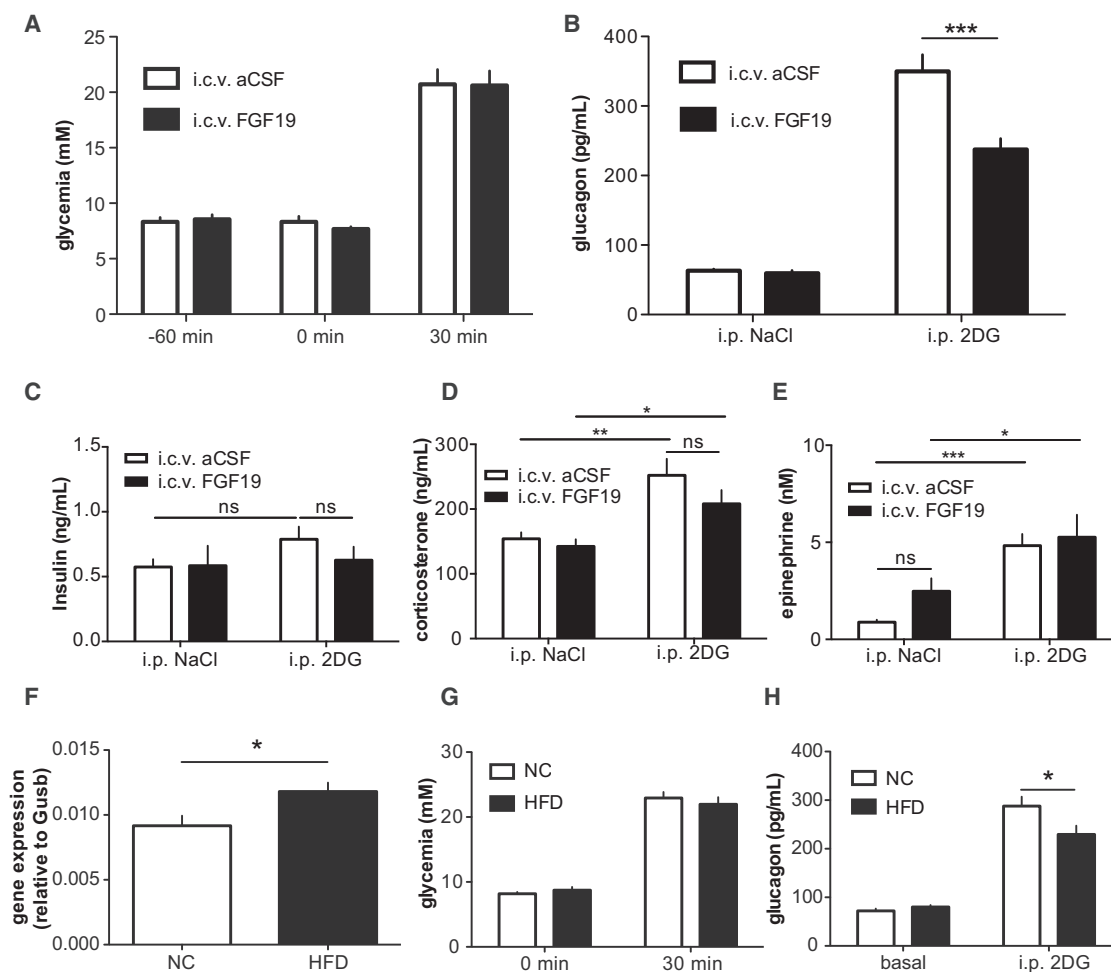


**Figure 3. Fgf19 and the Control of Glucagon Secretion**

(A) Glycemia of mice injected i.c.v. with aCSF or FGF19 60 min before i.p. injection (0 min) of 2DG (600 mg/kg) (n = 7). (B) Plasma glucagon 30 min after i.p. injection of saline or 2DG in mice that were treated 60 min before with i.c.v. injection of aCSF or FGF19 (n = 7). (C–E) Plasma insulin (C), corticosterone (D), and epinephrine (E) 30 min after i.p. injection of saline or 2DG in mice that were treated 60 min before with i.c.v. injection of aCSF or FGF19 (n = 9–10) (E). (F) Hypothalamic expression of *Fgf15* in C57Bl6/J mice fed a NC or a HFD for 4 weeks (n = 6–8). (G) Glycemia in NC and HFD fed mice before and 30 min after i.p. injection of 2DG (n = 6–8). (H) Plasma glucagon in NC and HFD fed mice in the basal state and 30 min after 2DG injection (n = 6–8). Data are mean ± SEM. \*p ≤ 0.05 and \*\*\*p ≤ 0.001. Two-way ANOVA followed by Bonferroni post hoc test (A–E, G, and H). Student's t test (F).

neuroglucopenia-induced glucagon secretion. Furthermore, i.c.v. delivery of FGF19 prevented the increase in vagal activity induced by neuroglucopenia, and this was associated with a reduced activation of DVC neurons. As i.c.v. FGF19 activates pERK1/2 only in hypothalamic ARC neurons, our data suggest that hypothalamic *Fgf15* modulates DVC activity in an indirect manner.

*Fgf15/19* belongs to the endocrine fibroblast growth factor family, which also includes *Fgf21* and *Fgf23* (Owen et al., 2015). *Fgf15/19* expression in ileal cells is induced by the bile acids released in the intestinal lumen in the postprandial state through activation of the bile acid nuclear receptor FXR (Inagaki et al., 2005). *Fgf15/19* binds to receptors consisting of *Fgfr1c* or *Fgfr4* and the co-receptor *klotho-beta* (Owen et al., 2015). In liver, *Fgf15/19* reduces bile acid synthesis through the inhibition

of *Cyp7a1* (Jung et al., 2007; Vergnes et al., 2013). It also induces glycogen synthesis through the activation of the Ras-Erk-p90RSK and inhibits gluconeogenesis via the CREB-PGC1 $\alpha$  pathway (Kir et al., 2011; Potthoff et al., 2011). *Fgf15/19* has more recently been described to affect body weight, glucose tolerance, and insulin sensitivity through a central action (Marcelin et al., 2013; Morton et al., 2013; Ryan et al., 2013).

Here, we found that *Fgf15* is also expressed in the hypothalamus through an unbiased search for genetic intervals associated with neuroglucopenia-induced glucagon secretion in recombinant inbred mice. Among the 128 genes present in the identified QTL of chromosome 7, RNA-seq analysis revealed that 11 of these genes were expressed in the hypothalamus and expression of *Fgf15*, and, of the large intergenic noncoding RNA (*linc*)

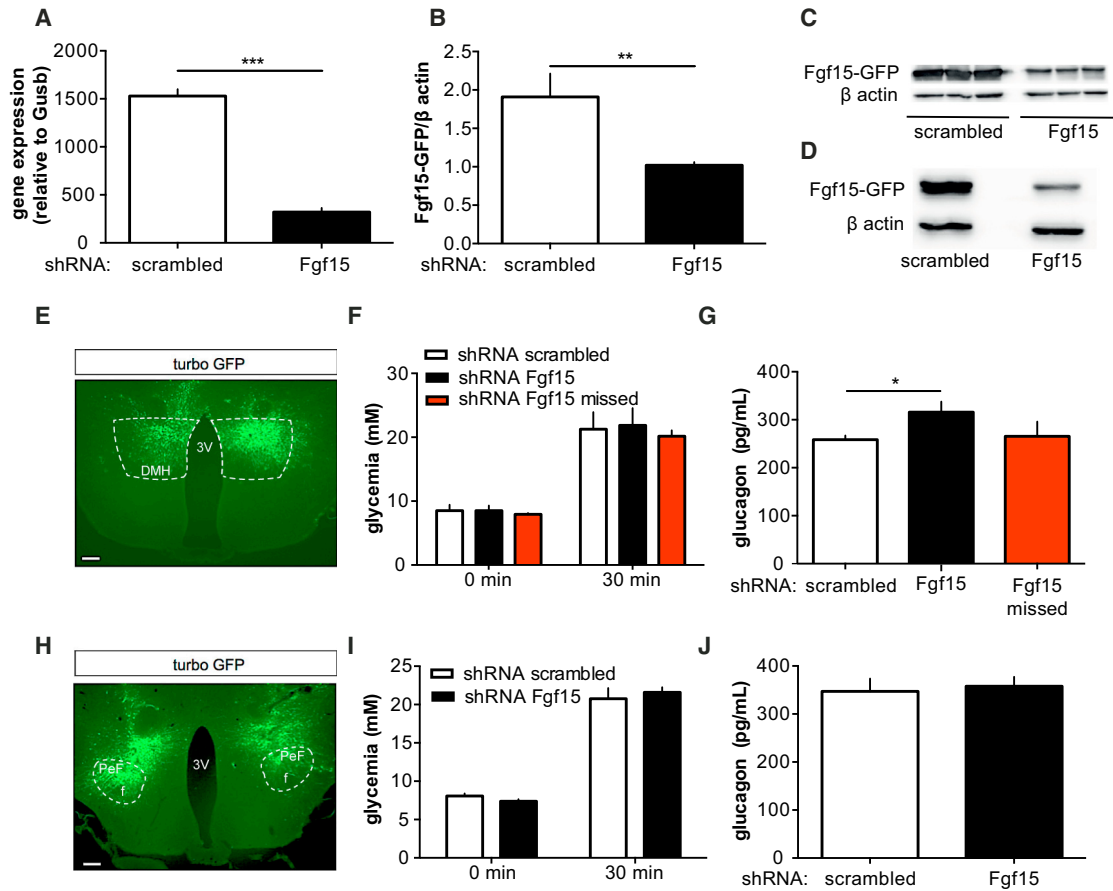


**Figure 4. *Fgf15* Silencing in the DMH Increases 2DG-Induced Glucagon Secretion**

(A) Silencing of *Fgf15* expression after co-transfection of HEK293T cells of an *Fgf15-GFP* cDNA with the selected *Fgf15*-specific shRNA encoding lentiviral vector (n = 3).

(B) Quantification of *Fgf15* protein expression in the same conditions as (A) (n = 3).

(C) Western blot analysis of *Fgf15* and β-actin expression quantitated in (B).

(D) Western blot analysis of *Fgf15* and β-actin expression in HEK293T cells infected with a control (scrambled) or an *Fgf15*-shRNA lentivirus and transfected with an *Fgf15-GFP* expression plasmid.

(E) Example of the correct bilateral injection in the DMH of *Fgf15*-shRNA lentiviruses. The scale bar represents 100 μm.

(F) Glycemia in mice injected in the DMH with control (scrambled) or *Fgf15*-shRNA lentiviruses before (0 min) and 30 min after i.p. injection of 2DG. missed: mice with incorrect *Fgf15*-shRNA encoding lentivirus injection sites. (n = 10–19).

(G) Plasma glucagon levels 30 min after 2DG i.p. injections (n = 10–19).

(H) Example of the correct bilateral injection in the PeF of *Fgf15*-shRNA lentiviruses. The scale bar represents 100 μm.

(I) Glycemia in mice injected in the PeF with control (scrambled) or *Fgf15*-shRNA lentiviruses before and 30 min after i.p. injection of 2DG (n = 12).

(J) Plasma glucagon levels 30 min after 2DG i.p. injections (n = 12).

Data are mean ± SEM. \*p ≤ 0.05; \*\*p ≤ 0.01; and \*\*\*p ≤ 0.001. Student's t test (A, B, and J). Two-way ANOVA followed by Bonferroni post hoc test (F and I). One-way ANOVA followed by Bonferroni post hoc test (G).

RNA-encoding, *Gm17685* showed the highest correlation with the glucagon trait. Expression levels of *Fgf15* and *Gm17685* were also highly positively correlated to each other. As lincRNAs are implicated in the control of gene expression through a variety of mechanisms (Zhao and Lin, 2015), it could be hypothesized that *Gm17685* plays a regulatory role in *Fgf15* expression. Testing this will, however, require future investigations.

To localize *Fgf15* expression in the brain, we used a highly sensitive and specific in situ hybridization technique. In the hypothalamus, expression of *Fgf15* was found in the PeF and in the DMH, and co-in situ hybridization analysis with the neuronal

marker *NeuN* revealed that it was expressed in neurons. No signal for *Fgf15* was identified in the DVC or in any other brainstem nuclei.

To assess whether central *Fgf15* could impact neuroglucopenia-induced glucagon secretion, we first injected i.c.v. FGF19 in C57BL/6 mice and tested the glucagon response to a subsequent i.p. injection of 2DG. We observed that i.c.v. FGF19 decreased the glucagon response induced by 2DG, in agreement with the results of the genetic screen. We also observed in a model of high fat diet feeding an association between overexpression of hypothalamic *Fgf15* and a decrease in

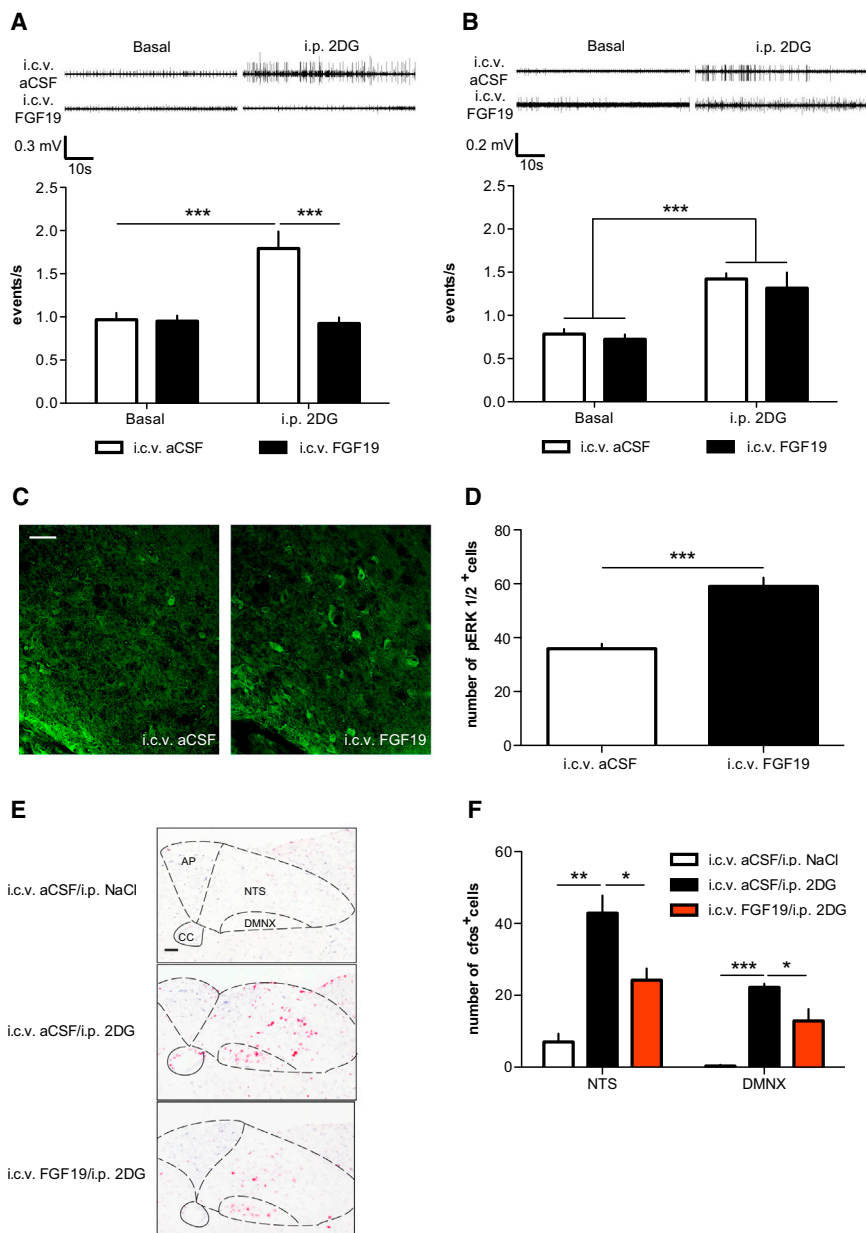


### Figure 5. FGF19 Blunts 2DG-Induced Parasympathetic Nerve Activity

(A) Parasympathetic nerve firing rate in the basal state and following i.p. 2DG injection in mice previously treated with i.c.v. aCSF or FGF19 (top: representative trace and bottom: quantification of the firing activity) (n = 6–7).

(B) Sympathetic nerve firing rate in the basal state and following i.p. 2DG injection in mice previously treated with i.c.v. aCSF or FGF19 (top: representative trace and bottom: quantification of the firing activity) (n = 7).

(C) Representative micrographs of pERK1/2 positive cells in the ARC 30 min after i.c.v. injection of aCSF or FGF19.

(D) Quantification of pERK1/2 positive cells in the ARC 30 min after i.c.v. injection of aCSF or FGF19. (n = 5–7).

(E) Representative micrographs of *c-fos* positive cells in NTS and DMNX at bregma –7.56 mm of mice that received i.c.v. aCSF and 60 min later i.p. NaCl (upper), i.c.v. aCSF and 60 min later i.p. 2DG (mid), or i.c.v. FGF19 and 60 min later i.p. 2DG (lower). area postrema, AP; central canal, CC; nucleus of the solitary tract, NTS; DMNX.

(F) Quantification of *c-fos* positive cells in NTS and DMNX of mice treated as in (E). The scale bar represents 50  $\mu$ m.

Two-way ANOVA followed by Bonferroni post hoc test (A and B). Student's t test (D). One-way ANOVA followed by Bonferroni post hoc test (F). \*p  $\leq$  0.05; \*\*p  $\leq$  0.01; and \*\*\*p  $\leq$  0.001. Data are mean  $\pm$  SEM.

Other studies have shown that i.c.v. FGF19 could improve glucose tolerance in HFD fed mice and ob/ob mice (Marcelin et al., 2013; Morton et al., 2013). In ob/ob mice, the effect of FGF19 on glucose tolerance was associated with an increase in insulin-independent glucose disposal and insulin sensitivity without changes in insulin secretion. Glucagon secretion was, however, only assessed following i.p. injection of FGF19 and was not modified by this treatment (Morton et al., 2013).

2DG-induced glucagon secretion, lending further support to the negative correlation between hypothalamic *Fgf15* and glucagon secretion. However, the most convincing evidence for a direct link between hypothalamic *Fgf15* expression and glucagon secretion comes for the shRNA-mediated silencing of *Fgf15*. This effect was observed when injection of the recombinant lentivirus was in the DMH, but not in the PeF. Because the PeF is a rather large structure, it is possible that our injections were not sufficiently extensive over the entire PeF structure to observe an effect. Nevertheless, the critical observation is that injection of the recombinant lentivirus in the DMH was sufficient to increase 2DG-induced glucagon secretion, establishing a direct link between *Fgf15* in this structure and the control of glucagon secretion.

Neuroglucopenia-induced glucagon secretion involves activation of the parasympathetic and sympathetic branches of the autonomic nervous system. During graded hypoglycemia development, the parasympathetic nerve is activated immediately when the glycemia falls under the  $\sim$ 5 mM and sympathetic activity is increased at lower glycemic levels (Taborsky and Mundinger, 2012). Here, we found that i.c.v. FGF19 dampens parasympathetic, but not sympathetic nerve activity during 2DG-induced neuroglucopenia, an observation that provides an explanation for the reduced glucagon secretion. Moreover, the observation that 2DG-induced-glucagon secretion was not completely blunted after i.c.v. FGF19 can be explained by the fact that the sympathetic activity was not affected by i.c.v. FGF19. This suggests that FGF19 specifically impairs the

parasympathetic activity to reduce glucagon secretion during neuroglucopenia.

The soma of the parasympathetic neurons is located within the DVC. The primary neurons activated by i.c.v. FGF19 and identified by immunofluorescence detection of pERK1/2 are, however, present in the ARC and not found in other hypothalamic or brainstem nuclei. This is in agreement with previous observations showing that FGF19 activates pERK1/2 in the ARC (Marcelin et al., 2013). Importantly, we found that i.c.v. FGF19 blunted 2DG-induced neuronal activation in the NTS and the DMNX as assessed by *c-fos* expression analysis. This therefore indicates that i.c.v. FGF19 can prevent activation of DVC neurons in response to neuroglucopenia, and our observations suggest that its action may be indirect through a first action on ARC neurons. This also provides an explanation for the dampening effect of i.c.v. FGF19 on neuroglucopenia-induced vagal activity.

Previous reports have shown that i.c.v. FGF19 induces pERK1/2 in NPY/AgRP neurons, but fails to induce *c-fos* in POMC neurons (Marcelin et al., 2013; Morton et al., 2013). Thus, NPY/AgRP neurons could be the primary target neurons of Fgf15 neurons of PeF and/or DMH, and these neurons may then negatively control DVC neurons in a pERK1/2-dependent manner. A role for the ARC and NPY/AgRP neurons in mediating the effects of Fgf15/19 can be supported by the fact that the melanocortin pathway has been shown to be necessary for the central effects of FGF19 on glucose tolerance (Marcelin et al., 2013; Morton et al., 2013). Whereas tracing approaches in mice expressing the Cre recombinase under the control of *Fgf15* promoter should be used to confirm these observations, our data provide a first insight in a *Fgf15*-dependent neural network, which involves an ARC/DVC pathway to regulate glucagon secretion during neuroglucopenia.

Together, our genetic screen combined with gene expression analysis provides compelling evidence that hypothalamic *Fgf15* is negatively involved in the control by neuroglucopenia of glucagon secretion. *Fgf15* is expressed by discrete subpopulations of neurons in the PeF and DMH and Fgf15/19 blunts vagal firing activity and dampens the response of the DVC neurons to 2DG-induced neuroglucopenia, a response that involves activation of pERK1/2 in ARC neurons. Collectively, these results, initiated by an unbiased search for novel genes involved in counterregulatory response to neuroglucopenia, reveal a new site of *Fgf15* expression and provide a mechanistic framework to elucidate Fgf15 action in the control of parasympathetic nervous activity and glucagon secretion. They may provide new insight into the neuronal control of counterregulation and its deregulation in the etiology of HAAF in type 1 and type 2 diabetic patients.

## EXPERIMENTAL PROCEDURES

### Mice

BXD mouse strains were purchased from the center of phenogenomics of EPFL (Lausanne). C57Bl6/J mice were purchased from Charles River Laboratories. Animals were housed on a 12 hr light/dark cycle and were fed a standard rodent chow diet (Diet 3436, Provimi Kliba) or a high-fat diet (235 HF, SAFE diets). Experiments were performed with 10- to 14-week-old male mice.

### Study Approval

All animal experimentations were approved by the Veterinary Office of Canton de Vaud.

### Biochemical Measurements

Blood was collected under isoflurane anesthesia. Glycemia was measured using a glucometer (Ascensia Breeze 2, Bayer Healthcare). Glucagon was quantitated by radioimmunoassay (Millipore, cat. number: GL-32K). ELISAs were used for insulin (cat. number: 10-1247-10, Mercodia), and corticosterone (cat. number: ADI-900-097, Enzo Life Sciences) measurements. Free plasma epinephrine was quantified as described (Dunand et al., 2013).

### Phenotyping of Glucagon Secretion in BXD Mice

BXD mice were handled daily for 2 weeks before the experiment. On the first experiment day, glycemia was taken at 9:00 a.m. and, if stable for 1 hr, the mice received at 10:00 am an i.p. injection of NaCl 0.9%. Blood was collected 30 min later for basal glucagon quantification. Mice were then allowed to recover for 2 weeks with daily handling. Then the same protocol was used with i.p. injection of 2DG (600 mg/kg).

### RNA-Seq Analysis

Total RNA extraction from hypothalamus and brainstem samples was performed using the peqGOLD TriFast method (PEQLAB). RNA were obtained from mice sacrificed during the morning in random fed conditions as for the QTL screening. RNA integrity was verified with a 2100 Bioanalyzer (Agilent). For each BXD strain, equal amounts of RNAs from 3 to 6 hypothalami were pooled in a final volume of 50  $\mu$ L. RNA-seq libraries were prepared using 1  $\mu$ g of pooled RNAs and the Illumina TruSeq Stranded mRNA reagents (Illumina) on a Sciclone liquid handling robot (PerkinElmer) using a PerkinElmer-developed automated script. Cluster generation was performed with the resulting libraries using the Illumina TruSeq SR Cluster Kit v3 reagents and sequenced on the Illumina HiSeq 2000 using TruSeq SBS Kit v3 reagents. Sequencing data were processed using the Illumina Pipeline Software version 1.82. A sequencing depth of 40 millions of reads using 100 bp single-end reads was used. Reads were mapped to the *mm9* genome with tophat (v. 2.0.8) using library-type = fr-firststrand. Other parameters were set by default. Count data for exons were generated using htseq-count from the HTSeq package (<http://www.huber.embl.de/users/anders/HTSeq/>, version 0.5.4p3) using RefSeq annotation, with parameters stranded = reverse and mode = union. The normalized read counts per gene were log transformed, and then Pearson correlation was used to calculate the correlation of gene expression with the physiological trait.

### QTL Mapping

GeneNetwork ([www.genenetwork.org](http://www.genenetwork.org)) variants data set comprising about 15,000 SNPs on the whole mouse genome was used to perform QTL mapping. Calling SNPs on our RNA-seq data have been used as a way to check for genetic drift in the BXD strains. SNP calling was performed using the Genome Analysis ToolKit from the Broad Institute (v. 3.2) using the recommended workflow for RNA-seq data. Variants were filtered using a quality threshold ( $>= 5,000$ ). Furthermore, genotypes with more than 10% missing information were also removed. This allowed tagging the discrepant variants—compared to our RNAseq experiments—as “unknown” (eight 0.05% genotypes per strain) for QTL analysis. Finally, variants similar to our SNP calling data were merged to remove redundant information. For QTL analysis, we used the *r/qtl* packages with Haley-Knott (HK) regression method. Pseudo-markers were generated at a density of 1 cM. QTL location was obtained with 1.5 LOD (6.915 LRS) support intervals as suggested previously (Broman and Sen, 2009). The significance and suggestive thresholds were computed with 2,000 permutations: the sequences of the various strains were shuffled 2,000 times and association recalculated at each permutation. This allowed calculating the probability to find these associations by chance.

### shRNA Selection and Lentivirus Production

To test the efficiency of the *Fgf15* shRNAs, an *Fgf15* cDNA was subcloned in frame with GFP in the pCMV6-AC-GFP plasmid (cat. number: MG202456, OriGene) and scrambled or *Fgf15*-targeted shRNAs were subcloned in the

pGFP-C-shLenti plasmid (cat. number: TL514099, OriGene). The vectors were co-transfected into HEK293T cells using lipofectamine 3000 (cat. number: L3000015, Thermo Fisher Scientific). At 48 hr later, total RNA and proteins were extracted and *Fgf15* expression was determined by qRT-PCR and protein by western blot. The selected shRNA sequence has the following sequence: 5'-GTCTGTGTCAGATGAAGATCCACTCTTTC-3'. Lentiviruses were produced as described (Salmon and Trono, 2006). Viral titers were evaluated by infection of HEK293T cells. The silencing efficacy of the *Fgf15*-shRNA lentivirus was tested in infected HEK293T cells that were transfected with *Fgf15* expression plasmid.

### Stereotaxy

Surgeries were performed under ketamine/xylazine anesthesia. Cannulas were placed in the lateral ventricle (−0.7 mm from the bregma; −1.3 mm from the midline; and −1.8 mm from the surface of the skull) (Paxinos and Watson, 1982). Lentiviruses (200 nL; 4.10<sup>9</sup> TU/mL) were injected in the DMH (−1.7 mm from the bregma; ± 0.35 mm from the midline; and −5.0 mm from the surface of the skull) and PeF (−1.7 mm from the bregma; ± 0.75 mm from the midline; and −5.15 mm from the surface of the skull) (Paxinos and Watson, 1982). Animals were allowed to recover for 1 week with daily handling and body weight monitoring after i.c.v. placement and for 2 weeks after lentivirus injections. The placement of the cannula was checked by histological analysis after blue ink delivery, and the sites of injection (GFP fluorescence) were verified on 40 μm brain sections.

### I.c.v. Injections

Mice received at 9:00 am on the test day either i.c.v. aCSF (125 mM NaCl, 2.5 mM KCl, 1.25 mM NaH<sub>2</sub>PO<sub>4</sub>, 1 mM MgCl<sub>2</sub>, 2 mM CaCl<sub>2</sub>, 26 mM NaHCO<sub>3</sub> and 12.5 mM sucrose, 300 mOsm, and pH = 7.4) or FGF19 (2.5 μg) (cat. number: cyt-700-b, Prospecbio). One hr later, mice were injected i.p. with NaCl 0.9% or 2DG 600 mg/kg. Blood and brains were collected 30 min later for quantification of glucagon secretion or for in situ hybridization detection of *c-fos*. For pERK1/2 detection, brains were dissected 30 min after i.c.v. delivery of either aCSF or FGF19.

### qRT-PCR

Tissues preparation, RNA extraction, and qRT-PCR were performed as described (Mounien et al., 2010). The following forward (F) and reverse (R) primers were used: fibroblast growth factor 15 (*Fgf15*) F5'-GAGGAC CAAAACGAACGAAATT-3' and R5'-ACGTCCTTGATGGCAATCG-3'; fibroblast growth receptor 1 isoform c (*Fgfr1c*): F5'-GGAGGTGCTTCATCTAC GGA-3' and R5'-AGAGTGATGGGAGAGTCCGA-3'; fibroblast growth receptor 4 (*Fgfr4*): F5'-GCCCGACAGTTCTTTTGA-3' and R5'- TTCCCAAAGCGGA TCGAGAG-3'; *klotho* beta (*Klotho beta*): F5'-CCTTCCCACTGGCAATCT GT-3' and R5'-GGGTGGTACAACGTCACCAT-3'; and beta-glucuronidase (*Gusb*): F5'-GTGATGGAGGAGCTGGTTTCG-3' and R5'-AGCAGAGGAGGCT CATTGG-3'. *Gusb* was used as a housekeeping gene to normalize gene expression in all experiments.

### Immunofluorescence Microscopy and In Situ Hybridization

For immunofluorescence detection of pERK1/2, mice were fixed by a transcardiac perfusion of 4% cold paraformaldehyde (PFA) in sodium phosphate buffer (0.1 M, pH 7.4). Brains were dissected and kept for 2 hr in PFA at 4°C before overnight incubation in sucrose 30% at 4°C and frozen at −80°C. There were 20 μm cryosections that were prepared, placed on glass slides, and incubated in a blocking buffer consisting of 0.1 M phosphate buffer pH 7.4 containing 3% of normal goat serum and 0.3% Triton X-100 for 1 hr, then with a rabbit monoclonal antibody directed against pERK1/2 (cat. number: 4370, 1/200, Cell Signaling) for 48 hr, and for 1.5 hr with an Alexa Fluor 488-conjugated goat anti-rabbit IgG (H+L) antibody (cat. number: 11008, 1/400, Life Technologies). Slides were mounted in Mowiol for fluorescence imaging. For pERK1/2 positive cells quantification, four different sections for each mouse were analyzed. For in situ hybridization analysis, the hypothalamus and brainstem were dissected using a mouse brain matrix with 1-mm section dividers (CellPoint Scientific); all tissues were fixed for 28 hr in 10% formalin before embedding in paraffin. There were 5 μm sections that were cut and in situ hybridization for *Fgf15*, *c-fos*, *NeuN*, and dihydrodi-

picolinate reductase (*DapB*) (cat. number: 412811, 316921, 313311, and 310043) was processed using the RNAscope and RNAscope 2.0 HD Red Detection Kit Assay (Advanced Cell Diagnostics). Double in situ hybridization was performed using RNAscope 2-Plex Assay (cat. number: 320701). Sections were counterstained with Mayer's hematoxylin, mounted using Aquatex mounting medium (cat. number: 363123S, VWR), and observed using an Axio Imager D1 (Zeiss) microscope interfaced with AxioVision software (Zeiss). Quantification of *c-fos* expression was performed on sections cut at bregma −7.56 mm from three different mice. Image analysis was performed using ImageJ.

### Autonomic Nervous System Activity Recording

The firing rates of the thoracic branch of both vagal and sympathetic nerves along the carotid artery were recorded as previously described (Magnan et al., 1999; Tarussio et al., 2014). Unipolar nerve activity was recorded continuously for 1 hr under isoflurane anesthesia (30 min during basal condition after i.c.v. aCSF/FGF19 and before i.p. 2DG and 30 min during 2DG-induced neuroglucopenia) using the LabChart 8 software (AD Instrument). Data were digitized with PowerLab 16/35 (ADInstruments). Signals were amplified 10<sup>5</sup> times and filtered using 200/1,000 Hz band pass filter. Firing rate analysis was performed using LabChart 8.

### Statistical Analysis

Data are expressed as mean ± SEM. Statistical analysis were performed using GraphPad Prism 5.0c, either by a one-way Anova followed by Bonferroni post hoc test, a two-way Anova followed by Bonferroni post hoc test, or by an unpaired two-tailed Student's t test when appropriate. p values less than 0.05 were considered significant.

### ACCESSION NUMBERS

The accession number for the raw data (Fastq files) for hypothalamus RNA-seq reported in this paper is Gene Expression Omnibus (GEO): GSE87586.

### AUTHOR CONTRIBUTIONS

B.T. conceived the project. A.P., J.S., and X.B. performed the phenotyping of glucagon secretion in BXD mice. A.P., F.B., M.J., and M.I. performed the QTL and RNA-seq analysis. A.P., X.B., and D.T. performed the experiments in C57Bl6/J mice and the in situ hybridization. S.Q. produced the recombinant lentiviruses. E.G. performed epinephrine analysis. A.P. and B.T. conceived the experimental design, analyzed the data, and wrote the paper. All the authors have approved the manuscript.

### ACKNOWLEDGMENTS

We thank Professor Paul Franken (UNIL, Lausanne) for very useful discussions and comments on the manuscript. We are grateful to Professor Rob Williams (Nashville, TN, USA) for allowing access to the BXD mice and to Professor Johan Auwerx and Dr. Evan Graehl Williams for expert advice. We thank Dr. Keith Harshman (Genomic Technology Facility, CIG) for outstanding support for RNA-seq analysis. This work was supported by grants to B.T. from the Swiss National Science Foundation (3100A0B-128657 and CRSII3-136201) and a European Research Council Advanced Grant (268946; INSIGHT).

Received: December 18, 2015

Revised: October 4, 2016

Accepted: October 13, 2016

Published: November 8, 2016

### REFERENCES

Alquier, T., Kawashima, J., Tsuji, Y., and Kahn, B.B. (2007). Role of hypothalamic adenosine 5'-monophosphate-activated protein kinase in the impaired counterregulatory response induced by repetitive neuroglucopenia. *Endocrinology* 148, 1367–1375.

- Andreux, P.A., Williams, E.G., Koutnikova, H., Houtkooper, R.H., Champy, M.F., Henry, H., Schoonjans, K., Williams, R.W., and Auwerx, J. (2012). Systems genetics of metabolism: the use of the BXD murine reference panel for multiscalar integration of traits. *Cell* 150, 1287–1299.
- Berthoud, H.R., Fox, E.A., and Powley, T.L. (1990). Localization of vagal preganglionics that stimulate insulin and glucagon secretion. *Am. J. Physiol.* 258, R160–R168.
- Broman, K.W., and Sen, S. (2009). *A Guide to QTL Mapping with R/qtl* (Springer).
- Burcelin, R., Crivelli, V., Dacosta, A., Roy-Tirelli, A., and Thorens, B. (2002). Heterogeneous metabolic adaptation of C57BL/6J mice to high-fat diet. *Am. J. Physiol. Endocrinol. Metab.* 282, E834–E842.
- Chan, O., and Sherwin, R. (2013). Influence of VMH fuel sensing on hypoglycemic responses. *Trends Endocrinol. Metab.* 24, 616–624.
- Chesler, E.J., Lu, L., Wang, J., Williams, R.W., and Manly, K.F. (2004). WebQTL: rapid exploratory analysis of gene expression and genetic networks for brain and behavior. *Nat. Neurosci.* 7, 485–486.
- Cryer, P.E. (2013). Mechanisms of hypoglycemia-associated autonomic failure in diabetes. *N. Engl. J. Med.* 369, 362–372.
- Dunand, M., Gubian, D., Stauffer, M., Abid, K., and Grouzmann, E. (2013). High-throughput and sensitive quantitation of plasma catecholamines by ultra-performance liquid chromatography-tandem mass spectrometry using a solid phase microwell extraction plate. *Anal. Chem.* 85, 3539–3544.
- Evans, M.L., McCrimmon, R.J., Flanagan, D.E., Keshavarz, T., Fan, X., McNay, E.C., Jacob, R.J., and Sherwin, R.S. (2004). Hypothalamic ATP-sensitive K<sup>+</sup> channels play a key role in sensing hypoglycemia and triggering counterregulatory epinephrine and glucagon responses. *Diabetes* 53, 2542–2551.
- Franken, P., Chollet, D., and Tafti, M. (2001). The homeostatic regulation of sleep need is under genetic control. *J. Neurosci.* 21, 2610–2621.
- Frizzell, R.T., Jones, E.M., Davis, S.N., Biggers, D.W., Myers, S.R., Connolly, C.C., Neal, D.W., Jaspan, J.B., and Cherrington, A.D. (1993). Counterregulation during hypoglycemia is directed by widespread brain regions. *Diabetes* 42, 1253–1261.
- Houtkooper, R.H., Mouchiroud, L., Ryu, D., Moullan, N., Katsyuba, E., Knott, G., Williams, R.W., and Auwerx, J. (2013). Mitonuclear protein imbalance as a conserved longevity mechanism. *Nature* 497, 451–457.
- Inagaki, T., Choi, M., Moschetta, A., Peng, L., Cummins, C.L., McDonald, J.G., Luo, G., Jones, S.A., Goodwin, B., Richardson, J.A., et al. (2005). Fibroblast growth factor 15 functions as an enterohepatic signal to regulate bile acid homeostasis. *Cell Metab.* 2, 217–225.
- Jackson, P.A., Cardin, S., Coffey, C.S., Neal, D.W., Allen, E.J., Penalzoza, A.R., Snead, W.L., and Cherrington, A.D. (2000). Effect of hepatic denervation on the counterregulatory response to insulin-induced hypoglycemia in the dog. *Am. J. Physiol. Endocrinol. Metab.* 279, E1249–E1257.
- Jung, D., Inagaki, T., Gerard, R.D., Dawson, P.A., Kliewer, S.A., Mangelsdorf, D.J., and Moschetta, A. (2007). FXR agonists and FGF15 reduce fecal bile acid excretion in a mouse model of bile acid malabsorption. *J. Lipid Res.* 48, 2693–2700.
- Karnani, M., and Burdakov, D. (2011). Multiple hypothalamic circuits sense and regulate glucose levels. *Am. J. Physiol. Regul. Integr. Comp. Physiol.* 300, R47–R55.
- Kir, S., Beddow, S.A., Samuel, V.T., Miller, P., Previs, S.F., Suino-Powell, K., Xu, H.E., Shulman, G.I., Kliewer, S.A., and Mangelsdorf, D.J. (2011). FGF19 as a postprandial, insulin-independent activator of hepatic protein and glycogen synthesis. *Science* 331, 1621–1624.
- Koutnikova, H., Laakso, M., Lu, L., Combe, R., Paananen, J., Kuulasmaa, T., Kuusisto, J., Häring, H.U., Hansen, T., Pedersen, O., et al. (2009). Identification of the UBP1 locus as a critical blood pressure determinant using a combination of mouse and human genetics. *PLoS Genet.* 5, e1000591.
- Lamy, C.M., Sanno, H., Labouëbe, G., Picard, A., Magnan, C., Chatton, J.Y., and Thorens, B. (2014). Hypoglycemia-activated GLUT2 neurons of the nucleus tractus solitarius stimulate vagal activity and glucagon secretion. *Cell Metab.* 19, 527–538.
- Levin, B.E., Becker, T.C., Eiki, J., Zhang, B.B., and Dunn-Meynell, A.A. (2008). Ventromedial hypothalamic glucokinase is an important mediator of the counterregulatory response to insulin-induced hypoglycemia. *Diabetes* 57, 1371–1379.
- Magnan, C., Collins, S., Berthault, M.F., Kassis, N., Vincent, M., Gilbert, M., Pénicaud, L., Ktorza, A., and Assimakopoulos-Jeannet, F. (1999). Lipid infusion lowers sympathetic nervous activity and leads to increased beta-cell responsiveness to glucose. *J. Clin. Invest.* 103, 413–419.
- Marcelin, G., Jo, Y.H., Li, X., Schwartz, G.J., Zhang, Y., Dun, N.J., Lyu, R.M., Blouet, C., Chang, J.K., and Chua, S., Jr. (2013). Central action of FGF19 reduces hypothalamic AGRP/NPY neuron activity and improves glucose metabolism. *Mol. Metab.* 3, 19–28.
- Marty, N., Dallaporta, M., and Thorens, B. (2007). Brain glucose sensing, counterregulation, and energy homeostasis. *Physiology (Bethesda)* 22, 241–251.
- McCrimmon, R.J., Shaw, M., Fan, X., Cheng, H., Ding, Y., Vella, M.C., Zhou, L., McNay, E.C., and Sherwin, R.S. (2008). Key role for AMP-activated protein kinase in the ventromedial hypothalamus in regulating counterregulatory hormone responses to acute hypoglycemia. *Diabetes* 57, 444–450.
- Miki, T., Liss, B., Minami, K., Shiuchi, T., Saraya, A., Kashima, Y., Horiuchi, M., Ashcroft, F., Minokoshi, Y., Roeper, J., and Seino, S. (2001). ATP-sensitive K<sup>+</sup> channels in the hypothalamus are essential for the maintenance of glucose homeostasis. *Nat. Neurosci.* 4, 507–512.
- Morton, G.J., Matsen, M.E., Bracy, D.P., Meek, T.H., Nguyen, H.T., Stefanovski, D., Bergman, R.N., Wasserman, D.H., and Schwartz, M.W. (2013). FGF19 action in the brain induces insulin-independent glucose lowering. *J. Clin. Invest.* 123, 4799–4808.
- Mounien, L., Marty, N., Tarussio, D., Metref, S., Genoux, D., Preitner, F., Foretz, M., and Thorens, B. (2010). Glut2-dependent glucose-sensing controls thermoregulation by enhancing the leptin sensitivity of NPY and POMC neurons. *FASEB J.* 24, 1747–1758.
- O'Malley, D., Reimann, F., Simpson, A.K., and Gribble, F.M. (2006). Sodium-coupled glucose cotransporters contribute to hypothalamic glucose sensing. *Diabetes* 55, 3381–3386.
- Owen, B.M., Mangelsdorf, D.J., and Kliewer, S.A. (2015). Tissue-specific actions of the metabolic hormones FGF15/19 and FGF21. *Trends Endocrinol. Metab.* 26, 22–29.
- Paxinos, G., and Watson, C. (1982). *The Rat Brain in Stereotaxic Coordinates* (Academic Press).
- Peirce, J.L., Broman, K.W., Lu, L., and Williams, R.W. (2007). A simple method for combining genetic mapping data from multiple crosses and experimental designs. *PLoS ONE* 2, e1036.
- Potthoff, M.J., Boney-Montoya, J., Choi, M., He, T., Sunny, N.E., Satapati, S., Suino-Powell, K., Xu, H.E., Gerard, R.D., Finck, B.N., et al. (2011). FGF15/19 regulates hepatic glucose metabolism by inhibiting the CREB-PGC-1 $\alpha$  pathway. *Cell Metab.* 13, 729–738.
- Ritter, S., Li, A.J., Wang, Q., and Dinh, T.T. (2011). Minireview: The value of looking backward: the essential role of the hindbrain in counterregulatory responses to glucose deficit. *Endocrinology* 152, 4019–4032.
- Rosen, G.D., Chesler, E.J., Manly, K.F., and Williams, R.W. (2007). An informatics approach to systems neurogenetics. *Methods Mol. Biol.* 401, 287–303.
- Routh, V.H. (2002). Glucose-sensing neurons: are they physiologically relevant? *Physiol. Behav.* 76, 403–413.
- Routh, V.H. (2010). Glucose sensing neurons in the ventromedial hypothalamus. *Sensors (Basel)* 10, 9002–9025.
- Ryan, K.K., Kohli, R., Gutierrez-Aguilar, R., Gaitonde, S.G., Woods, S.C., and Seeley, R.J. (2013). Fibroblast growth factor-19 action in the brain reduces food intake and body weight and improves glucose tolerance in male rats. *Endocrinology* 154, 9–15.
- Salmon, P., and Trono, D. (2006). Production and titration of lentiviral vectors. In *Current Protocols in Neuroscience*, J.N. Crawley, ed. (John Wiley & Sons). <http://dx.doi.org/10.1002/0471142901>.

- Stanley, S., Domingos, A.I., Kelly, L., Garfield, A., Damanpour, S., Heisler, L., and Friedman, J. (2013). Profiling of glucose-sensing neurons reveals that GHRH neurons are activated by hypoglycemia. *Cell Metab.* *18*, 596–607.
- Steinbusch, L., Labouèbe, G., and Thorens, B. (2015). Brain glucose sensing in homeostatic and hedonic regulation. *Trends Endocrinol. Metab.* *26*, 455–466.
- Taborsky, G.J., Jr., and Mundinger, T.O. (2012). Minireview: The role of the autonomic nervous system in mediating the glucagon response to hypoglycemia. *Endocrinology* *153*, 1055–1062.
- Tarussio, D., Metref, S., Seyer, P., Mounien, L., Vallois, D., Magnan, C., Foretz, M., and Thorens, B. (2014). Nervous glucose sensing regulates postnatal  $\beta$  cell proliferation and glucose homeostasis. *J. Clin. Invest.* *124*, 413–424.
- Thorens, B. (2012). Sensing of glucose in the brain. *Handbook Exp. Pharmacol.* *209*, 277–294.
- Unger, R.H., and Orci, L. (1981). Glucagon and the A cells: physiology and pathophysiology. *N. Engl. J. Med.* *304*, 1518–1524.
- Verberne, A.J., Sabetghadam, A., and Korim, W.S. (2014). Neural pathways that control the glucose counterregulatory response. *Front. Neurosci.* *8*, 38.
- Vergnes, L., Lee, J.M., Chin, R.G., Auwerx, J., and Reue, K. (2013). Diet1 functions in the FGF15/19 enterohepatic signaling axis to modulate bile acid and lipid levels. *Cell Metab.* *17*, 916–928.
- Wong, N., Morahan, G., Stathopoulos, M., Proietto, J., and Andrikopoulos, S. (2013). A novel mechanism regulating insulin secretion involving Herpud1 in mice. *Diabetologia* *56*, 1569–1576.
- Zhao, X.Y., and Lin, J.D. (2015). Long noncoding RNAs: a new regulatory code in metabolic control. *Trends Biochem. Sci.* *40*, 586–596.